A numerical study on the feasibility of a cable and pipeline decommissioning device

Martinelli, M.; Pisanò, F.; Korndorffer, D.

DOI
10.3723/JLEG6121

Publication date
2023

Document Version
Final published version

Published in
Offshore Site Investigation Geotechnics 9th International Conference Proceeding

doi:10.3723/JLEG6121

A numerical study on the feasibility of a cable and pipeline decommissioning device

M. Martinelli
Deltares, Delft, The Netherlands

F. Pisanò
TUDelft, Delft, The Netherlands

D. Korndorffer
Enersea, The Netherlands

ABSTRACT: The decommission of cables or pipelines is a vital aspect which ensures a sustainable and effective process of the infrastructure life cycle. Ideally, all offshore installations and equipment should be removed entirely but, in some cases, some flexibility is provided by the international (or national) laws or regulations whether the total removal might induce extreme risk, cost, or adverse environmental damage. The development of technology that facilitates pipeline or cable decommissioning is of vital importance. A newly developed concept of a decommissioning tool has just proposed by Enersea. This novel tool is placed into the pipeline (or over the cables) and induces vibrations in the structure and the surrounding soils, which result in a lower uplift resistance of the pipeline or cable. This paper presents the feasibility study of this technique for a cable/pipeline buried in sand. It is illustrated if it is possible to induce soil liquefaction in the vicinity of the buried pipeline/cable, and the length of the pipeline affected by the liquefiable zone is also presented.

1 Introduction

In general, used pipelines are left in situ after service life. Nevertheless, modern environmental regulations require that pipelines, umbilicals and cables, after service life, are periodically inspected or completely removed from the seabed. The first option incurs relatively small but recurring costs, while the latter option involves a significant one-time expense. It is worth noting that contaminated pipelines, such as for example those contaminated with mercury, are required to be removed.

One factor for the large costs is that heavy equipment is required to access and lift buried pipelines. Heavy equipment requires the mobilisation of larger and more expensive vessels. Pipelines up to 16” must be buried in the Dutch sector of the North Sea, with a typical burial depth of 1 meter or more. The soil cover is problematic for the removal of the pipelines. While it is possible to pull the pipeline through a minimal amount of cover, the pipeline will likely fail under the load required. It is thus required to remove the cover on the pipeline. The removal of cover through either mechanical means or jetting requires powerful equipment and is a slow process.

To reduce the costs associated with pipeline or cable removal a new approach is needed. Enersea has recently developed a concept for a tool that aims to reduce soil resistance through induced vibrations, which would make pipeline removal easier/faster – and therefore less expensive. The objective of this system is to have a cost-effective subsea decommissioning solutions with the least amount of environmental impact for the recovery of (contaminated) subsea buried pipelines and cables, reducing companies decommissioning liabilities and enabling the recovery of valuable materials (copper, duplex, etc).

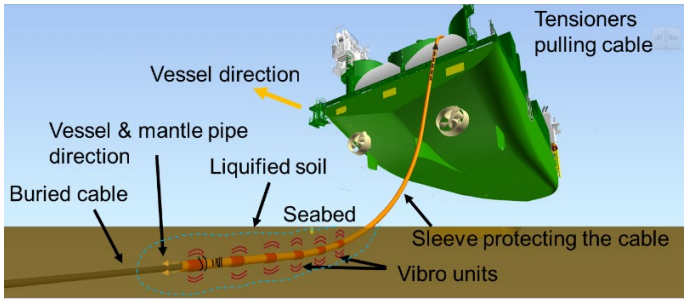

Figure 1: Sketch of the decommissioning device analysed in this study – application to buried cables.

The envisioned installation procedure is the following: (1) the soil cover on top of the pipeline or cable will be removed by lowering the sleeve and vibro-unit in vertical position; (2) the vibro-units will be activated liquefying the soil, and the water flow inside the sleeve will remove the soil and uncover the pipeline/cable; (3) the pipeline/cable will be cut at onside of the trench. For what concerns the cable, a A&R wire is send through the sleeve (yellow) and connected to a Chinese finger holding the end of the cut cable. Then the cable can be pulled through the sleeve and the tensioner will be engaged.

In the envisioned design, one or multiple vibrating units would be used to induce either full (or partial) soil liquefaction around the pipeline, as illustrated in Figure 1. The Electro or hydraulic power will be generated on board of the vessel and distributed through the sleeve anulus (pipe-in-pipe configuration) toward the vibro units. The vibro unit will be set up as groups or even individual sub-assemblies providing redundancy to the deburial process.

The pipeline decommissioning tool proposed by Enersea is a solution that has not been previously used by the offshore industry (a patent application is currently under review), and could potentially be applied also to cable extraction operations in relation to offshore wind farming. In order to assure that the proposed decommissioning solution is both technically viable and financially beneficial, more insight needs to be gained into vibratory soil-pipeline interaction, particularly into the hydro-mechanical mechanisms (build-up and dissipation of pore pressures) that, supposedly, would facilitate the extraction of a buried pipeline (or cable).

This paper illustrates a methodology which is able to answer the following questions:

1. *Is it possible to induce soil liquefaction in the vicinity of a buried pipeline/cable using the proposed decommissioning tool?*
2. *How long it should be expected to take for soil liquefaction to occur?*
3. *How far from the pipeline/cable it will be possible to induce soil liquefaction?*
4. *How much reduction of the extraction force may be achieved by liquefying the soil around the pipeline/cable? With what influence of the burial depth?*

2 Methodology

The numerical analysis of pipeline vibratory extraction in water-saturated soil appears at a first glance as a very complex problem. The following factors contribute to such complexity:

- the problem is intrinsically three-dimensional (3D), dynamic, and fully coupled (in that pipeline vibrations affect the response of the surrounding soil, which in turn constrains the motion of the pipeline);
- the hydro-mechanical behaviour of soils is highly non-linear, especially in the presence of cyclic/dynamic loading conditions, for which it is necessary to reproduce phenomena such as cyclic pore-pressure build-up (possibly leading to liquefaction) and strain accumulation, as well as intrinsic dependency of stiffness and strength on effective stress state, loading history, stress path and rate, etc.;
- full extraction of a buried pipeline is per se a large deformation problem, which should in principle be simulated by resorting to modern numerical methods overcoming the typical assumption of small-deformation modelling;
- from a computational standpoint, the combination of 3D conditions and relatively high loading frequencies (i.e., larger than 20 Hz) would require the use of finely discretised numerical models, both in space and time, which very quickly leads to computations of unbearable cost.

For the purpose of this first feasibility study, a number of simplifications have been introduced to enable an engineering representation of the phenomena at hand, yet believed to bear sufficient resemblance to reality – it is advised, however, that more stringent validation against real experimental data is pursued in the future.

In more detail, the problem has been tackled as follows:

- in lieu of a complete 3D model, the combination of two uncoupled/simpler models has been adopted, namely a 1D pipeline-soil interaction model (section 3.1) and a 2D model of a pipeline cross-section interacting with the surrounding soil (section 3.2). Both sub-models have been set up by accounting the fully dynamic conditions (i.e., including the influence of inertial effects).
- the 1D model has been used to model the pipeline vibrations (and their propagation in space and time) induced by the aforementioned decommissioning device. The soil-structure interaction effects have been simulated by introducing lumped viscoelastic elements (impedance) to represent transient soil reactions. The main difficulty about the setup of the 1D model is the calibration of soil impedance parameters (particularly to represent liquefied soil conditions), which is aided by the second (2D) model.
- after obtaining an estimate of the vibratory pipeline displacements, detailed dynamic soil-structure analyses have been performed using the continuum 2D model of a pipeline cross-section interacting with water-saturated soil (in this study, exclusively sand). The 2D simulation results enable thorough assessment of pore pressure effects around a pipeline cross-section, which is instrumental to (i) refining initial estimates of soil impedance and (ii) assessing possible reduction of pipe uplift capacity – both matters are intimately related to vibration-induced pore pressure build-up.

Overall, the above framework decomposes the full three-dimensionality of the reference soil-structure interaction problem into two uncoupled schemes that are geometrically simpler – therefore, easier to handle computationally.

3 Model set-up and parameter calibration

The following reference specifications have been adopted in this study:

- steel pipeline of outer diameter and thickness equal to 35.56 cm and 1.905 cm, respectively;
- steel Young's modulus equal to 210 GPa and Poisson's ratio equal to 0.2;
- length of the vibrating unit equal to 25 cm;
- 5 kg rotating mass, with eccentricity and rotation frequency equal to 9 cm and 50 Hz, respectively.
- the reference setup features two counter-rotating vibro-units in the same device, producing overall a purely vertical harmonic force;
- pipeline buried at 1.0 m depth in loose sand, with a relative density of 35%.

3.1 *1D analysis of dynamic pipeline-soil interaction*

This approach studies the response of the pipeline in space and time, with discrete soil interaction elements.

The reference geometry of the 1D model is illustrated in Figure 2, where the 1D steel pipeline structure is discretised using 2-node Euler-Bernoulli beam finite elements of 25 cm each. The vibrating unit is defined as a single point source of imposed harmonic loading – located in Figure 2 between points 3 and 4, approximately 5 m from point 3 – and it applies a nodal harmonic force $F(t) = F_{max}\, e^{i\omega t}$ (with ω circular frequency) with F_{max} = 88.8 kN and frequency f = $\omega/2\pi$ = 50 Hz.

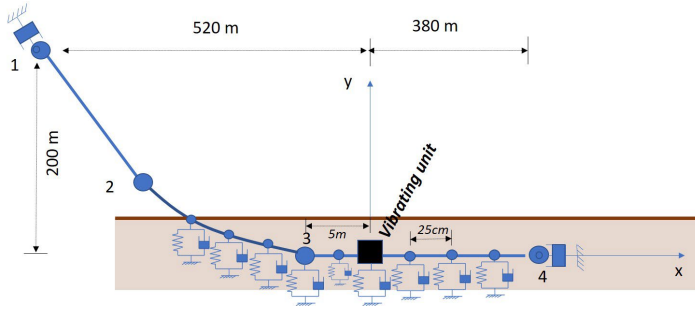

Figure 2: Geometry of the 1D pipeline-soil model.

The pipeline segment 1-4 in Figure 2 is endowed with absorbing boundaries (viscous dashpots) at the two end nodes 1 and 4, following the well-established approach by Lysmer and Kuhlemeyer (1969). This choice has enabled the simulation of an infinite pipeline length beyond node 4, while above node 1 has avoided explicit modelling of the connection with the vessel.

In the spirit of 1D soil-structure interaction modelling, dynamic soil reactions at embedded pipeline nodes (see Figure 2) have been reproduced using lumped visco-elastic Kelvin-Voigt interaction elements, whose behaviour is completely characterised by the values of the static elastic stiffness, K_{stat}, and the viscosity parameter, C. An additional mass, m_{add}, has been added to each embedded pipeline node to obtain the correct dynamic soil stiffness at the considered loading frequency – further details on this aspect may be found in Gazetas (1991). Due to the non-linearity of soil behaviour, these values may vary significantly with the loading magnitude, which governs the extent of the pore pressure build-up and inelastic (plastic) straining in the soil. Therefore, realistic ranges of K_{stat} and C values have been identified through detailed 2D analyses.

The numerical integration in space and time of the 1D model has been performed using in-house software developed at Deltares. Particularly, the well-known Newmark time integration algorithm has been adopted in combination with a non-dissipative, second-order accurate pair of integration parameters, i.e., $\alpha = 0.5$ and $\beta = 0.25$ (Hughes, 2012).

The type of output produced by the numerical program is qualitatively illustrated in Figure 3 and depicts how induced pipeline vibration would propagate from the vibrating unit towards the (infinitely far) end of the pipeline. The simulated response to a harmonic input force ($F(t) = F_{max}\, e^{i\omega t}$) is represented by the distribution in space and time of the pipeline displacement, $u(x, t) = U_{max}(x)e^{i(\omega t - \phi)}$. Given the linearity of the pipeline structural behaviour, also the displacement response is expected to be harmonic, with amplitude $U_{max}(x)$ decreasing with the distance x from the vibrating unit, the same circular frequency ω as the input force, and a phase lag ϕ.

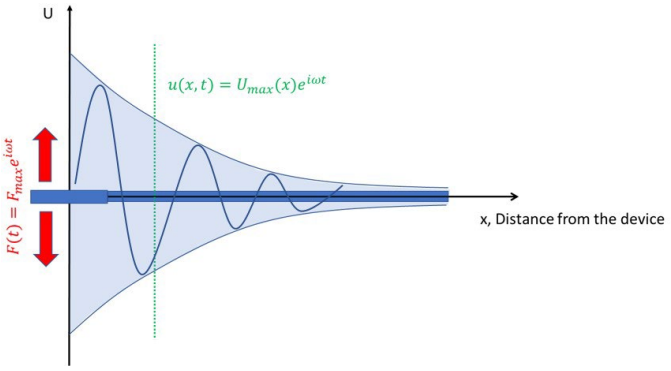

Figure 3: Qualitative pipeline response returned by the 1D model under a harmonic point load.

3.2 *2D analysis of dynamic pipeline-soil interaction*

This approach studies the response of the pipeline in time at a selected cross-section, with continuum soil modelling.

3.2.1 *Numerical model and boundary conditions*

Figure 4 shows the geometry and the space discretisation (FE mesh) adopted for the 2D soil-pipe model interaction model and representing a pipeline cross-section buried 1.0 m below the seabed. Given the geometrical and loading symmetries of the system under consideration (exclusively undergoing vertical vibrations), it has been possible to reduce the

computational burden of 2D simulations by modelling only half of the domain (2.5 m × 3.0 m).

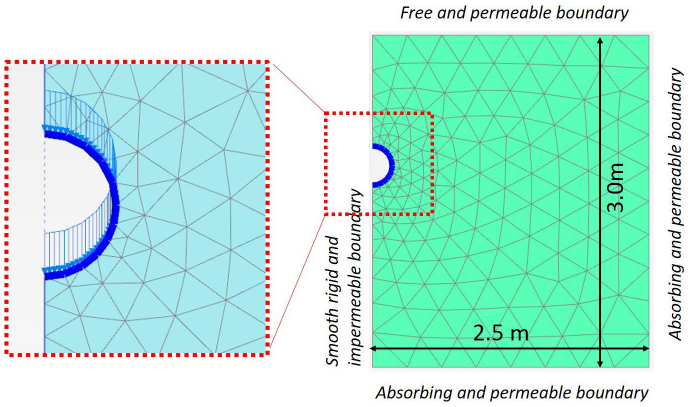

Figure 4: Geometry and FE mesh of the 2D pipeline-soil model

The free surface at the top represents the seabed and has been set as a perfectly permeable boundary; the left boundary (along the symmetry axis of the full 2D model) has been fixed along the orthogonal direction and let free to displace vertically (smooth rigid boundary), with no allowance for pore water flow (impermeable boundary); the bottom and right boundaries are fully permeable with imposed pore pressure values (free field conditions, sufficiently far from the pipe cross-section) and can mitigate spurious wave reflections back into the domain using the well-known viscous wave absorption approach by Lysmer and Kuhlemeyer (1969).

The point load applied in the corresponding 1D model has been represented as a vertical distributed load uniformly applied along the circumference of the cross-section. Its magnitude has been obtained for each simulation case as $q_{max} = F_{max}/(\pi D \times 1\ m)$, where D is the outer diameter of the pipeline cross-section.

3.2.2 *Constitutive model for soil liquefaction*

The total unit weight of the soil has been set to γ = 19 kN/m^3, while the value of 10^{-5}m/s has been assumed for the (isotropic) hydraulic conductivity.

The behaviour of water-saturated sand subjected to cyclic loading has been simulated in 2D soil-pipe interaction analyses using the PM4Sand model (Boulanger and Ziotopoulou, 2013, Ziotopoulou and Boulanger, 2013).

The necessary soil parameters have been calibrated to reproduce the Groningen-specific liquefaction triggering curve (Green et al., 2020) (i.e., the relationship between number of cycles to liquefaction, N, and corresponding cyclic stress amplitude, CSR), and the post-liquefaction response (in terms of cyclic strain accumulation against the number of cycles while loading cycles are applied around vanishing mean effective stress) (Tasiopoulou et al., 2020).

3.2.3 *Numerical analyses*

The following three different types of numerical analyses have been performed for each considered geometrical/loading scenario:

1. **DynFC-FullyC**, i.e., *dynamic, force-controlled, fully coupled analysis* (with soil consolidation). Simulation of pipe-soil interaction accounting for the (competing) build-up and dissipation of pore pressures in response to pipeline vibrations. This analysis option has been adopted to serve two distinct goals: (1) determining the steady-state soil stress field that is later used to determine the uplift resistance of the pipeline; (2) calculating at the considered cross-section the dynamic impedance of the pipeline-soil system, which is needed to calibrate the lumped visco-elastic soil elements adopted in the 1D model.
2. **QSDC-Drained**, i.e., *quasi-static (no inertiae), displacement-controlled, drained analysis*. Simulation of static pipe-soil interaction (no inertial effects) to determine the ultimate uplift resistance of of the pipeline at the considered cross-section. This type of analysis has been performed after the completion of the fully coupled dynamic analysis (DynFC-FullyC analysis). To this end, a vertical displacement of 10 cm has been applied to the pipeline cross-section to achieve ultimate capacity conditions and determine the corresponding reaction force. Drained conditions (no pore pressure build-up) have been assumed for this type of analysis, under the assumption that an uplift mechanism in permeable sand would not produce appreciable excess pore pressures (i.e., in excess with respect to their hydrostatic values). Prior to the QSDC-Drained analysis, a calculation step with nil external loads has been performed in order to achieve fully balanced stress conditions in the soil's solid skeleton after the conclusion of the DynFC-FullyC analysis.
3. **QSDC-Undrained**, i.e., *quasi-static (no inertiae), displacement-controlled, undrained analysis.* Simulation of cyclic pipeline-soil interaction at the considered cross-section to determine the secant static stiffness (K_{stat}) of the lumped interaction elements in the 1D model. Accordingly, the cross-section has been set to follow an imposed vertical cyclic displacement, so as to obtain the corresponding force reaction (not affected by the inhibited inertial terms) and, ultimately, the secant stiffness K_{stat} (in principle evolving with number of loading cycles). This kind of simulations have been repeated multiple times to compute K_{stat} for different values (order of magnitude) of the applied cyclic displacement. Undrained conditions (no pore water flow, constant soil

skeleton volume) have been assumed to exclude the interplay of soil permeability and loading frequency, which would have required additional parametric studies – it should be noted, however, that vibrations at the considered loading frequency are likely to produce nearly (if not fully) undrained behaviour.

4 Numerical results

4.1 *Cross-section response from 2D simulations*

DynFC-FullyC analyses have been performed to simulate a physical time period of 1 second, which has been verified to be sufficient for the attainment of steady state vibrations at 50 Hz. It should be noted that, in light of the plain strain assumption, the 2D analysis would tend to overestimate the vibratory displacement predicted by a 3D model featuring the same harmonic load per unit length – due to the fact that the 2D idealisation corresponds with assuming a vibratory source of infinite length along the pipeline. Therefore, a heuristic relationship has been considered between the Fmax values used in the 2D calculations and the maximum force applied by the Vibrating Unit, with the sole requirement of inducing in the 2D model a harmonic displacement larger than the value returned by the 1D model (where the correct F_{max}=88 kN has been applied). Since, vibrations of decreasing amplitude are expected at increasing distance from the vibratory source, the effect of a lower loading amplitude has been quantified by re-computing the response of the system for lower values of the external force – i.e., after multiplying F_{max} by a scaling factor fact lower than 1.0.

The use of the 2D model has enabled the determination of (1) the uplift resistance after the 1 second vibration at 50 Hz, and (2) the constitutive parameters of lumped soil elements that govern the response of 1D pipeline model – by varying *fact*, both (1) and (2) have been obtained as a function of the vibratory load magnitude.

4.1.1 *Simulation of soil's stress field and pipeline's uplift resistance*

Figure 5 shows the distribution of soil's vertical effective stress around the pipeline at different times during the vibrational stage (DynFC-FullyC calculations). Large excess pore pressures appear in the vicinity of the pipeline, with an area of influence ranging from 1 to 2 pipe diameters. Such a perturbation develops quite rapidly after the activation of the vibrating unit, and a nearly steady state is already reached after about 5-10 cycles (i.e., after 0.2-0.4 seconds).

At the end of the DynFC-FullyC calculation, i.e. after 1 second, the uplift resistance has been calculated thorugh a QSDC-Drained analysis – see results in Figure 6. Since the distribution of the excess pore pressure is not perfectly steady in time (it varies around an average value as a result of the induced vibrations), two distinct time instants have been selected within the same loading cycle to compute, by averaging, the drained bearing capacity, namely at 1.0 second and 1.01 second – the corresponding uplift curves are illustrated in Figure 6 (orange and blue dotted lines). As it may be expected, differences in the starting pore pressure distribution significantly affect the uplift response (particularly the stiffness) in the early stage of loading, though with a much lesser impact on the ultimate capacity – the resulting uplift resistance (per unit length, $R_{u,w/oVU}$) is in both cases of approximately 1.8 kN/m.

To quantify the effect (and effectiveness) of the pre-uplift vibrations, a similar QSDC-Drained analysis has been repeated for the case of hydrostatic initial distribution of pore pressure in the soil. In this case, a much larger uplift resistance ($R_{u,wVU}$) of approximately 9 kN/m has been obtained. An uplift resistance factor has then been defined as follows – ratio between the uplift resistance values obtained for the cases with and without vibrating unit:

$$URF = \frac{R_{u,w/oVU}}{R_{u,wVU}} \quad (1)$$

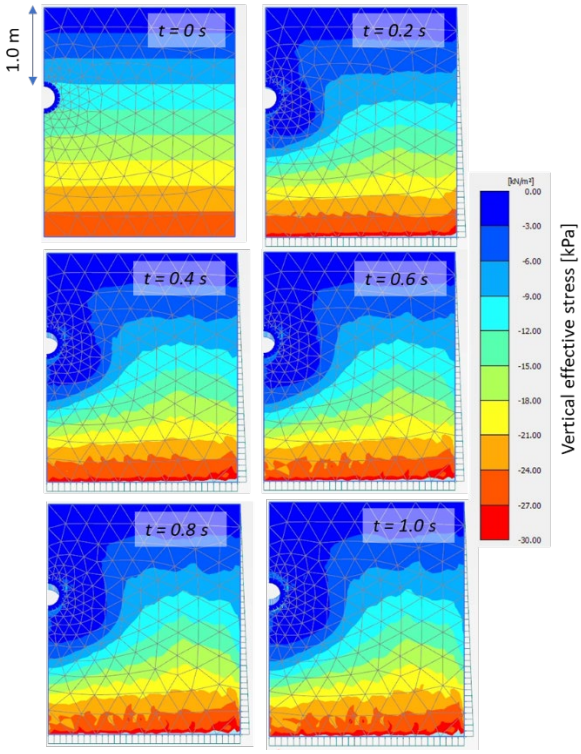

Figure 5: 2D DynFC-FullyC results associated with a load scaling factor fact = 1.0. Vertical stress distribution at different times.

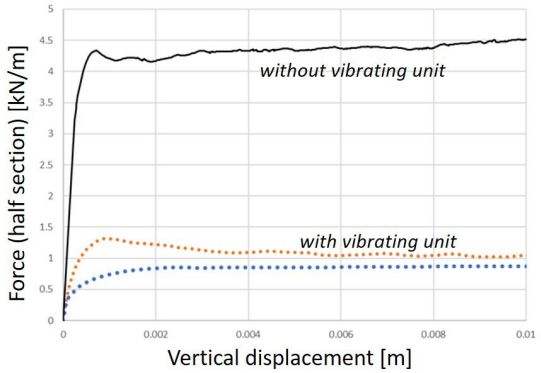

Figure 6: Effect of the vibrating unit on the uplift resistance. Stress field calculated using a scaling factor equal to fact = 1.0.

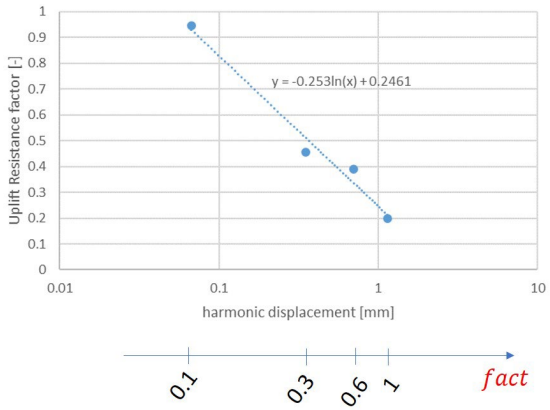

Figure 7: Effect of the vibration amplitude on the uplift resistance – 2D FE results and semi-logarithmic regression.

Figure 7 shows how URF varies with the value of the loading factor (fact), which is directly correlated with the corresponding value of the harmonic displacement (U_{max} – induced by the vibrating unit, see Figure 3). For further elaboration purposes it has appeared convenient to derive the following regression line from the plot in Figure 7:

$$URF_{1m} = -0.253 \cdot ln\,(Umax) + 0.2461 \qquad (2)$$

4.1.2 *Static stiffness and dynamic impedance*

The motion of the pipeline cross-section embedded into the soil can generally be described by the following momentum equation with lumped parameters:

$$\left(m_p + m_{add}\right)\ddot{u} = F(t) - K_{stat}\,u(t) - C\dot{u}(t) \qquad (3)$$

where $F(t)$ is the harmonic force acting on the pipeline cross-section, $u(t)$ the (harmonic) displacement, K_{stat} the secant static stiffness (defined for a given cycle), C the viscosity parameter of the dashpot, and mp the mass of the pipeline. The term m_{add} is a fictitious mass term that is necessary to correctly represent the dynamic stiffness of the coupled pipeline-soil system.

The dynamic impedance (K^*) is defined as the ratio between the force acting on the pipeline ($F(t)$) and the corresponding harmonic displacement ($u(t)$) under dynamic conditions (Gazetas, 1991):

$$K^* = K_{stat} - \omega^2\left(m_p + m_{add}\right) + i\omega C \qquad (4)$$

where Equation (4) has been exploited to express K^* as a function of K_{stat}, C, $m_p + m_{add}$ and the loading (circular) frequency ω (i denotes the imaginary unit, i = $\sqrt{-1}$). Accordingly, the dynamic stiffness (K_{dyn}) is defined as:

$$K_{dyn} = K_{stat} - \omega^2 m_{add} + i\omega C \qquad (5)$$

hence the following expression of the impedance results:

$$K^* = K_{dyn} - \omega^2 m_p + i\omega C \qquad (6)$$

The static secant stiffness K_{stat} has been calculated through QSDC-Undrained simulations, for different values of the vertical cyclic displacement, u_{cyc}. Relevant results are illustrated in Figure 9, where K_{stat} can be seen to decrease with the cyclic displacement amplitude. To confirm results reliability, it is worth noting that the obtained values of K_{stat} have been found to be well within the range provided by Guha et al. (2016) and NEN (2021). The work of Guha et al. provides an estimate of K_{stat} as a function of the small-strain shear modulus of the soil, whereas the Dutch standard provides operational values for soil-structure-interaction problems (NEN, 2021). Following this validation check, a power-law regression has also been performed for the results plotted in Figure 8:

$$K_{stat} = 8513.6\,u_{cyc}^{-0.496} \qquad (7)$$

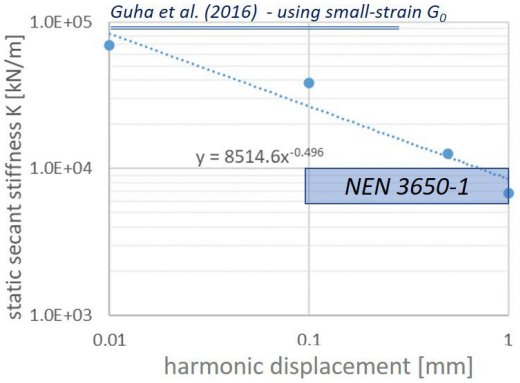

Figure 8: Relationship between (lunmped) secant static stiffness K_{stat} and pipeline's cyclic displacements u_{cyc} – 2D FE results and power-law regression.

Finally, m_{add} and C values have been obtained through the following simple steps:

1. the results of the DynFC-FullyC simulations have been processed to directly obtain the dynamic impedance K^* as per its definition given above;
2. the dashpot viscosity coefficient has been computed as $C = im(K^*)/\omega$, where $im(K^*)$ denotes the imaginary part of the dynamic impedance (which is in general a complex number);
3. the dynamic stiffness has been determined as $K_{dyn} = real(K^*) + \omega^2 m_p$, where $real(K^*)$ is the real part of the complex impedance;
4. the term m_{add} has been identified as:

$$m_{add} = \frac{K_{dyn} - K_{stat}}{\omega^2}$$

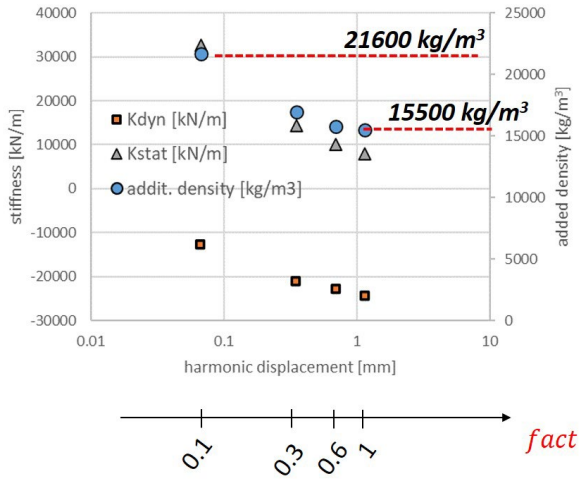

Figure 9: Values of madd, K_{stat} and K_{dyn} as a function the harmonic displacement U_{max} induced by different vibratory load magnitudes

At the end of the above step procedure, the identified value of m_{add} has directly been added to the mass of the pipeline in the 1D model. To this end, the pipeline density (ρ) has been increased by the term ($\rho_{add} = m_{add}$ / A , where A is the cross-section area of the pipeline) and, accordingly, the total mass density updated $\rho_{total} = \rho + \rho_{add}$.

Figure 9 shows the values of the additional density ρ_{add} as function of the harmonic displacements (u_{cyc}) induced in the dynamic analyses, using different values of the scaling factor fact. The same has been done for the viscosity parameter C – see Figure 10.

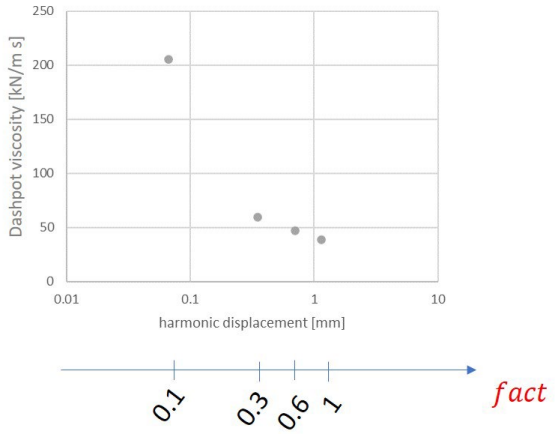

Figure 10: Values of the dashpot viscosity C as a function the harmonic displacement U_{max} induced by different vibratory load magnitudes.

4.2 *Pipeline response from 1D simulations*

Relevant input values for 1D pipeline analyses include K_{stat}, C, and ρ_{add} – all calibrated based on the results reported in Figures 12-13 as a function the harmonic displacement Umax induced by different vibratory load magnitudes on the pipeline cross-section. These input values strongly depend on the value of U_{max} generated by the vibratory process: therefore, an iterative process (where the lumped parameters at each node are adjusted as a function of the actual U_{max} value at the considered node) should in principle be performed to obtain a 1D response that is at the same time accurate and fully consistent with 2D results. However, in this first feasibility study, uniform input parameters have been set along the whole pipeline model, focusing on the two bounding cases associated with fact equal to 0.1 and 1.0, respectively. The former (*fact* = 0.1) is meant to represent the ideal case of intact soil (negligible strength reduction due to pore pressure), while the latter (*fact* = 1.0) corresponds with the case of substantial soil liquefaction occurred around the pipeline cross-section.

Representative 1D model results are illustrated in Figure 11 and Figure 12, where the amplitude of the harmonic displacement and the corresponding uplift resistance factor (*URF*) are developed in front of the vibrating unit. The results in Figure 12 should be more representative of the conditions experienced by the soil in the immediate vicinity of the vibrating unit, which is where the largest harmonic displacement occurs. Conversely, Figure 11 can describe accurately the response of the intact soil, as one would expect to find at a large distance from the vibratory source.

Overall, it may be observed that the presence of the vibrating unit (VU) generates a decrease in the uplift resistance by a factor approximately equal to 2 in the vicinity of the VU. The length of the pipeline segment that may benefit from such a decreased uplift resistance ranges, for the considered reference case, from 6 m (intact soil case, Figure 11) to over 25 m (liquefied soil case, Figure 12). Reality is believed to lie closer to the 6 m lower bound, although more realistic results could be obtained by accounting for the spatial variability of the soil impedance along the pipeline – this effect has been neglected herein for the sake of simplicity, where the "real" value tends to be closer to 6 m.

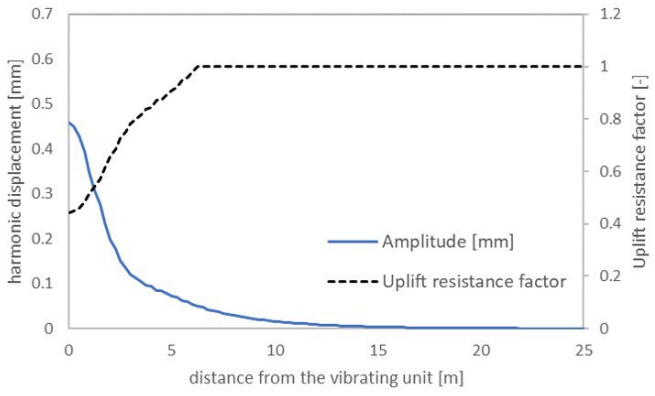

Figure 11: 1D model response for the case of intact soil (i.e., with *fact* = 0.1) – negligible pore pressure effects. Amplitude of the harmonic displacement U_{max} and *URF* value along the pipeline length.

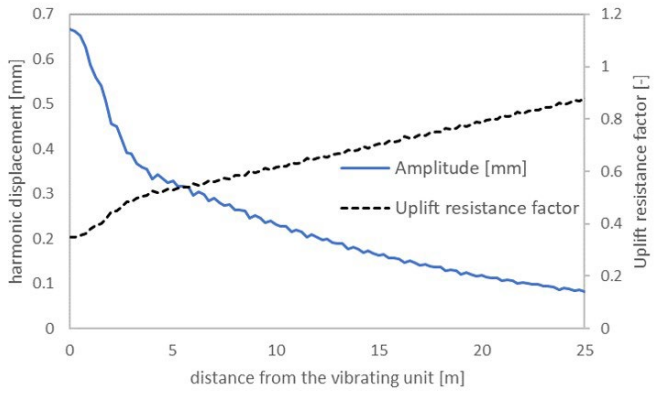

Figure 12: 1D model response for the case of liquefied soil (i.e, with *fact* = 1.0). Amplitude of the harmonic displacement U_{max} and *URF* value along the pipeline length.

5 Conclusions

This numerical study provides some evidence about the potential effectiveness of the examined new pipeline decommissioning method. Its physical foundation appears to be sound from a geotechnical standpoint and promising for full scale application.

At the same, however, an accurate quantification of the benefits that such a method could bring to the market is mandatory prior to further development and commercialisation.

The current methodology is used to answer the following research questions:

1. *Is it possible to induce soil liquefaction in the vicinity of a buried pipeline/cable using the proposed decommissioning tool?* Answer: Yes, it is theoretically possible, as long as the vibrating unit is able to mobilise "sufficient" displacement of the pipeline along the length where lower soil resistance is needed.
2. *How long it should be expected to take for soil liquefaction to occur?* Answer: Given the use of a high-frequency vibratory source (herein assumed to be at 50 Hz), steady-state conditions (including liquefaction, if all the other conditions allow it) will be achieved within fractions of second – it will be generally a fast process that can quickly adapt to the gradual extraction of consecutive pipeline segments. In denser sand (not considered in this study), larger number of cycles are expected to produce sufficient pore pressure build-up – in this case, the weakening of the soil manifests itself in the gradual accumulation of deviatoric strains (so-called cyclic mobility) rather than sudden liquefaction instability.
3. *How far from the pipeline/cable it will be possible to induce soil liquefaction?* Answer: The answer strongly depends on vibratory load magnitude and soil's hydro-mechanical properties (relative density, stiffness, and permeability). For the cases considered herein, an extension of the liquefied area up to 5-6 m down the location of the vibrating unit seems to be possible.
4. How much reduction of the extraction force may be achieved by liquefying the soil around the pipeline/cable? With what influence of the burial depth? Answer: In the vicinity of the vibrating unit, it may go up to 75% in the most favourable cases – then less reduction is predicted to take place as farther locations are considered. Along with all material/loading properties, the burial depth is expected to play an important role.

6 References

Boulanger, R. and Ziotopoulou, K. (2013). Formulation of a sand plasticity plane-strain model for earthquake engineering applications, *Soil Dynamics and Earthquake Engineering 53: 254–267*.

Gazetas, G. (1991). Formulas and charts for impedances of surface and embedded foundations, *Journal of Geotechnical Engineering 117(9): 1363–1381*.

Green, R., Bommer, J., Stafford, P., Maurer, B., Kruiver, P., Edwards, B., Rodriguez-Marek, A., de Lange, G., Oates, S., Storck, T. et al. (2020). Liquefaction hazard in the Groningen region of the Netherlands due to induced seismicity, *Journal of Geotechnical and Geoenvironmental Engineering 146(8)*.

Guha, I., Randolph, M. F. and White, D. J. (2016). Evaluation of elastic stiffness parameters for pipeline–soil interaction, *Journal of Geotechnical and Geoenvironmental Engineering 142(6)*: 04016009.

Hughes, T. J. (2012). *The finite element method: linear static 2and dynamic finite element analysis*, Courier Corporation.

Lysmer, J. and Kuhlemeyer, R. L. (1969). Finite dynamic model for infinite media, *Journal of the Engineering Mechanics Division 95(4): 859–877*.

NEN (2021). NEN 3650-1:2020 en: Requirements for pipeline systems - part 1: General requirements.

Tasiopoulou, P., Ziotopoulou, K., Humire, F., Giannakou, A., Chacko, J. and Travasarou, T. (2020). Development and implementation of semiempirical framework for modeling postliquefaction shear deformation accumulation in sands, *Journal of Geotechnical and Geoenvironmental Engineering 146(1): 04019120–04019120*.

Wang, D., Bienen, B., Nazem, M., Tian, Y., Zheng, J., Pucker, T. and Randolph, M. F. (2015). Large deformation finite element analyses in geotechnical engineering, *Computers and Geotechnics 65: 104–114*.

Ziotopoulou, K. and Boulanger, R. (2013). Calibration and implementation of a sand plasticity plane strain model for earthquake engineering applications, *Soil Dynamics and Earthquake Engineering 53: 268–280*.